CEO Clinical and Experimental Otorhinolaryngology Vol. 16, No. 4: 342-358, November 2023 https://doi.org/10.21053/ceo.2023.00668
pISSN 1976-8710 eISSN 2005-0720

Original Article

A Novel *EYA1* Mutation Causing Alternative RNA Splicing in a Chinese Family With Branchio-Oto Syndrome: Implications for Molecular Diagnosis and Clinical Application

Anhai Chen[1,2,3,*] · Jie Ling[4,*] · Xin Peng[3,5] · Xianlin Liu[1,2,3] · Shuang Mao[1,2,3] · Yongjia Chen[1,2,3] · Mengyao Qin[1,2,3] · Shuai Zhang[1,2,3] · Yijiang Bai[1,2,3] · Jian Song[1,2,3] · Zhili Feng[6,7] · Lu Ma[7,8] · Dinghua He[9] · Lingyun Mei[1,2,3] · Chufeng He[1,2,3] · Yong Feng[1,6,7,9]

[1]*Department of Otorhinolaryngology, Xiangya Hospital, Central South University, Changsha, China*
[2]*Key Laboratory of Otolaryngology Major Disease Research of Hunan Province, Changsha, China*
[3]*National Clinical Research Centre for Geriatric Disorders, Department of Geriatrics, Xiangya Hospital, Central South University, Changsha, China*
[4]*Medical Functional Experiment Center, School of Basic Medicine, Central South University, Changsha, China*
[5]*Department of Pathology, Xiangya Hospital, Central South University, Changsha, China*
[6]*Department of Otorhinolaryngology, Head and Neck Surgery, The Affiliated Changsha Central Hospital, Hengyang Medical School, University of South China, Changsha, China*
[7]*MOE Key Lab of Rare Pediatric Diseases and Institute of Otorhinolaryngology, Head and Neck Surgery, University of South China, Changsha, China*
[8]*The Hengyang Key Laboratory of Cellular Stress Biology, Institute of Cytology and Genetics, Hengyang Medical School, University of South China, Hengyang, China*
[9]*Department of Otorhinolaryngology, The Affiliated Maternal and Child Health Hospital of Hunan Province, Hengyang Medical School, University of South China, Changsha, China*

Objectives. Branchio-oto syndrome (BOS) primarily manifests as hearing loss, preauricular pits, and branchial defects. *EYA1* is the most common pathogenic gene, and splicing mutations account for a substantial proportion of cases. However, few studies have addressed the structural changes in the protein caused by splicing mutations and potential pathogenic factors, and several studies have shown that middle-ear surgery has limited effectiveness in improving hearing in these patients. BOS has also been relatively infrequently reported in the Chinese population. This study explored the genetic etiology in the family of a proband with BOS and provided clinical treatment to improve the patient's hearing.

Methods. We collected detailed clinical features and peripheral blood samples from the patients and unaffected individuals within the family. Pathogenic mutations were identified by whole-exome sequencing and cosegregation analysis and classified according to the American College of Medical Genetics and Genomics guidelines. Alternative splicing was verified through a minigene assay. The predicted three-dimensional protein structure and biochemical experiments were used to investigate the pathogenicity of the mutation. The proband underwent middle-ear surgery and was followed up at 1 month and 6 months postoperatively to monitor auditory improvement.

Results. A novel heterozygous *EYA1* splicing variant (c.1050+4 A>C) was identified and classified as pathogenic (PVS1(RNA), PM2, PP1). Skipping of exon 11 of the *EYA1* pre-mRNA was confirmed using a minigene assay. This mutation may impair EYA1-SIX1 interactions, as shown by an immunoprecipitation assay. The EYA1-Mut protein exhibited cellular mislocalization and decreased protein expression in cytological experiments. Middle-ear surgery significantly improved hearing loss caused by bone-conduction abnormalities in the proband.

Conclusion. We reported a novel splicing variant of *EYA1* in a Chinese family with BOS and revealed the potential molecular pathogenic mechanism. The significant hearing improvement observed in the proband after middle-ear surgery provides a reference for auditory rehabilitation in similar patients.

Keywords. *Hearing Loss; EYA1; Alternative Splicing; Correction of Hearing Impairment*

• Received May 12, 2023
Revised October 6, 2023
Accepted October 11, 2023

• Corresponding author: **Chufeng He**
Department of Otorhinolaryngology, Xiangya Hospital, Central South University, Changsha 410008, Hunan, China
Tel: +86-731-83428888, Fax: +86-731-85667618, Email: hechufeng2013@163.com

• Co-Corresponding author: **Yong Feng**
Department of Otorhinolaryngology, Head and Neck Surgery, The Affiliated Changsha Central Hospital, Hengyang Medical School, University of South China, Changsha 410008, Hunan, China
Tel: +86-731-83428888, Fax: +86-731-85667618, Email: fengyong_hn@hotmail.com

*These authors contributed equally to this study.

INTRODUCTION

Branchio-oto syndrome (BOS; MIM 602588) is an autosomal dominant disorder mainly characterized by hearing loss (HL), preauricular pits, and branchial fistulas. Patients with these symptoms and additional renal anomalies are diagnosed with branchio-oto-renal syndrome (BORS; MIM 113650) [1]. Collectively, these two diseases are referred to as branchio-oto-renal spectrum disorders due to a genetic overlap and shared similar morphologic characteristics [2]. Otological anomalies are the most frequent lesions in BOS/BORS, including malformations of the preauricular fistula, external ear (microtia, external ear canal anomaly), middle ear (ossicular chain anomaly) and inner ear (cochlear hypoplasia) structures, which could eventually lead to conductive, sensorineural or mixed-type HL, usually bilateral [3]. The prevalence of BOS/BORS is 1/40,000; it mainly occurs in European populations and has been reported less often in Asian populations [4,5].

Several causative genes have been identified in BOS/BORS, including *EYA1, SIX1*, and *SIX5*, accounting for approximately 40%, 4%, and 5% of the affected population, respectively [6]. The most common disease-causing gene, *EYA1*, encodes the transcriptional cofactor protein EYA1, which is highly conserved across species, is located on chromosome 8q13.3, and consists of 18 exons. The EYA1 protein can be translocated to the nucleus by interacting with the SIX1 protein, and this translocation plays an essential role in regulating the development of cranial sensory neurogenesis and craniofacial morphogenesis in mammals [7-9]. Genetically defective Eya1 mice exhibit otological phenotypes and HL similar to those of BOS/BORS. In total, 252 *EYA1*-related mutations have been reported, of which 189 are associated with BOS/BORS (http://www.hgmd.cf.ac.uk/, last updated January 2023). According to our previous systematic review, the *EYA1* gene has a variety of pathogenic mutation types, among which frameshift and splicing mutations predominate, followed by nonsense mutations, missense mutations, deletions, and complex rearrangements [10]. Although hundreds of variants have been found in patients with pathogenic variants of the *EYA1* gene, no hotspot mutations have been identified. Following the study by Song et al. [11], the alteration of crucial protein domains and potential causative factors resulting from *EYA1* splicing mutations have received less attention.

The clinical diagnosis of BOS/BORS was defined by Chang et al. [12], and this diagnostic pathway has been widely accepted as a way to help physicians distinguish BOS/BORS patients from those with other syndromic deafness disorders. An accurate diagnosis is based on meeting at least three major criteria (HL, preauricular pits, branchial anomalies, and renal anomalies), two major criteria and at least two minor criteria (external, middle, and inner ear anomalies; preauricular tags; facial asymmetry), or one major criterion with a first-degree relative who has the disease. BOS/BORS is a highly heterogeneous disorder clinically, as inconsistent clinical phenotypes (e.g., with or without renal abnormalities) have been observed among patients carrying the same mutation within a family, as well as significant differences in the phenotype or severity of HL [3,13]. Mixed HL is the most common type, accounting for 50% of patients, followed by conductive HL in 30% and sensorineural HL in 20%, unlike other types of syndromic-related HL, such as Waardenburg syndrome or Stickler syndrome [14,15]. Considering the structural anomalies of the middle ear that are common in BOS/BORS, auditory rehabilitation surgery may effectively improve hearing function [16]. However, several studies have reported unsatisfactory postoperative hearing outcomes [11,16,17].

Here, we collected data from three generations of a Chinese BOS family, performed middle-ear tympanoplasty on Patient III-1, and followed up on hearing improvement at 1 month and

HIGHLIGHTS

- We identified a novel splicing mutation of *EYA1* in three generations of a Chinese family with branchio-oto syndrome and reported its resultant aberrant splicing pattern.
- The novel *EYA1* mutation c.1050+4 A>C may impair the EYA1-SIX1 protein interaction due to aberrant RNA splicing, resulting in mislocalization and poor expression of the EYA1 protein.
- Middle-ear surgery for hearing rehabilitation achieved significant improvement in hearing in the proband with branchio-oto syndrome.

6 months after surgery. Using whole-exome sequencing (WES), a novel EYA1 splicing mutation, c.1050+4 A>C, was identified in the patients (I-1, II-2, III-1, III-3) but not in unaffected individuals in the family. A minigene assay was used to identify aberrant pre-mRNA splicing caused by c.1050+4 A>C, resulting in the skipping of exon 11 of *EYA1*. Furthermore, we found that the mutant EYA1 protein presented decreased protein stability and abnormal cellular sublocalization, which may result in the impairment of normal protein function and the occurrence of BOS.

MATERIALS AND METHODS

Ethics statement

This study was approved by the Medical Ethics Committee of Xiangya Hospital Central South University (No. 202106096), which was conducted after obtaining written informed consent from each subject or the parents of patients who were younger than 18 years old.

Research subjects and clinical examination

We analyzed the patients from three generations of an autosomal dominant inheritance family (Fig. 1A). The patients within the family were clinically diagnosed with BOS according to the criteria proposed by Chang et al. [12]. The auditory function examination was performed by a competent physician and involved pure tone audiometry (PTA; Madsen Orbiter-922) and acoustic conduction (GSI-33). Renal function was assessed by blood tests, and urinary system structural anomalies were assessed by urological ultrasound. In addition, a physical examination of the external ear and craniofacial and branchial regions was performed to diagnose any abnormalities, such as microtia, fistula, craniofacial deformities and other clinical manifestations.

Surgical treatment

Otic endoscope-assisted tympanoplasty surgery was carried out under general anesthesia in the proband. An intra-auricular incision was made during the operation, the "U"-shaped flap of the external auditory canal was separated from the fibrous tympanic ring, and the tympanic membrane was lifted to expose the structure of the tympanum. The integrity and functional status of the middle-ear structures, such as the ossicular chain, were carefully examined, and the incus was removed. A partial ossicular replacement prosthesis (PORP) artificial auditory bone (KURZ 1002226) was placed above the stapes to reconstruct the ossicular chain and achieve type II tympanoplasty.

Whole-exome sequencing

The detailed methods for the WES and bioinformatics approaches have been described previously [18]. WES was performed on the two patients (III-1, II-2) and a normal family member (III-3) on the Illumina paired-end 150 bp platform (Illumina) using SureSelect (V6 Kit, Agilent) to enrich the target DNA fragment (150 bp paired-end mode and 100x coverage) and capture all coding exons and flanking region sequences. The raw sequenced read qualities were assessed and filtered to acquire effectively sequenced data. The effectively sequenced reads were aligned to the human reference genome GRCh37/hg19 (UCSC version) by Burrows-Wheeler Aligner software (v0.7.8-r455) [19]. The aligned variants were ranked and called via SAMtools [20]. ANNOVAR software (v2017June8) was used to further annotate the called single-nucleotide variants (SNVs) and insertions and deletions (InDels) [21]. DNA from participating family members was extracted from peripheral blood lymphocytes with standard extraction procedures.

Sanger sequencing

Sanger sequencing was used to verify candidate variants to determine whether they were cosegregated in family members with HL. Primer pairs amplifying products within 1,000 bp were designed with the Primer3Plus online program (https://primer3plus.com/). The genomic DNA samples of each member together with the primer pairs were used to amplify the genomic regions of interest, and the polymerase chain reaction (PCR) products were further purified by agarose gel electrophoresis. The purified products were sequenced on an ABI 3730XL DNA analyzer (Thermo Fisher Scientific). Sequencing data were analyzed using SnapGene software (v6.0.2).

Three-dimensional protein structure

The three-dimensional (3D) structure of the EYA1 and SIX1 entire protein were predicted using AlphaFold v2.0. The EYA1-SIX1 protein docking structural models were further simulated using AlphaFold Multimer software with default settings [22]. The optimal model for the protein–protein binding site was visualized and analyzed with PyMOL software (v2.1). Protein-protein interface area were calculated using PDBePISA (www.ebi.ac.uk/pdbe/pisa).

Western blotting and nucleoplasm separation experiment

The cell protein was extracted from the residue using RIPA lysis buffer containing protease inhibitor cocktail (K1007, APE×BIO) and phosphatase inhibitor cocktail 1/2 (K1015, APE×BIO), and the samples were lysed at 4 °C for 30 minutes. The concentration of extracted protein was measured by a bicinchoninic acid assay kit (20201ES76, YEASEN), and the protein lysate was denatured by boiling with sodium dodecyl sulphate (SDS) loading buffer for 15 minutes. The cytoplasmic protein was harvested with CEA lysis buffer (10 M/L HEPES, 10 M/L KCl) containing protease inhibitor cocktail and phosphatase inhibitor cocktail 1/2 and lysed at 4 °C for 15 minutes. The nuclear protein was extracted from the above residue using CEB lysis buffer (CEA lysis buffer +1% SDS). The precipitated proteins (20 μg) were resolved on

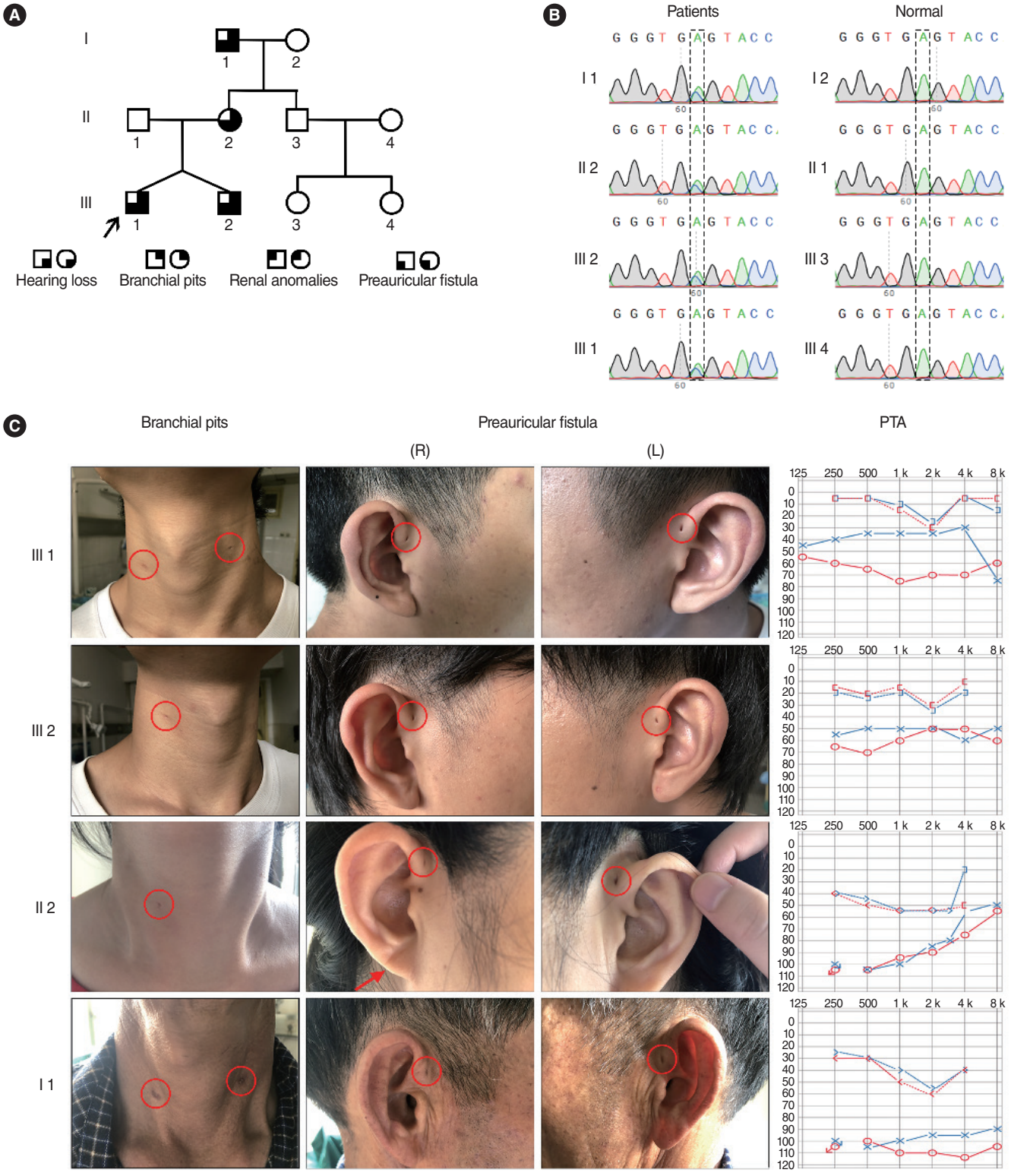

Fig. 1. Pedigree, Sanger sequencing, and clinical characteristics. (A) Pedigree of a branchio-oto syndrome (BOS) family with an autosomal dominant inheritance pattern. Square, male; circle, female. The black arrow indicates the proband, and the different quarter-filled symbols represent different phenotypes. (B) Sanger sequencing of the novel mutation *EYA1* c.1050+4 A>C in the available family subjects. The black dotted boxes indicate the novel mutation. (C) Clinical features of hearing loss and preauricular and branchial anomalies of four BOS patients. The red circle marks the location of the preauricular and branchial fistulas. The red arrow indicates the right earlobe agenesis of patient II-2. PTA, pure tone audiometry.

an 8% SDS-polyacrylamide gel and then transferred onto polyvinylidene fluoride (PVDF) membranes, which were further blocked with 10% skim milk powder at room temperature for 1 hour and incubated with primary antibody at 4 °C overnight. Primary antibodies for Western blotting were as follows: antibody against Flag (Abmart Cat# M20008), antibody against β-actin (Sigma Cat# A5441), antibody against GAPDH (Proteintech Cat# 60004-1-Ig) as a marker for cytoplasmic fraction, antibody against H3 (Proteintech Cat# 17168-1-AP) as a marker for nuclear fraction, antibody against SIX1 (Proteintech Cat# 10709-1-AP), β-tubulin (Abmart Cat# M20005). The band images were digitally captured and quantified by enhanced chemiluminescence (ChemiDoc MP Imaging System, Bio-Rad) after incubation with horseradish peroxidase-conjugated anti-mouse or anti-rabbit secondary antibodies.

Minigene assay

We obtained wild-type and mutant *EYA1* gene fragments using the genomic DNA of the patients and normal family members. A pair of primers was designed for an overlapping extension by nested PCR to amplify the target fragments. The PCR products and the pcMINI vector (Bioeagle Biotech Company) were digested with the restriction enzymes Kpn I and EcoR I and then ligated into the same restriction sites to generate the recombinant plasmids pcMINI-*EYA1*-WT/Mut. HeLa cells (CRL-3216, ATCC) and 293T cells (CCL-2, ATCC) were transiently transfected with the pcMINI-*EYA1*-WT/Mut plasmids using NeoFect DNA transfection reagent (NeoFect Biotech Company) according to the manufacturer's instructions and cultured in Dulbecco's modified eagle medium (DMEM)/high glucose containing 10% fetal bovine serum (FBS) at 37 °C with 5% CO_2. RNA was extracted by the two-step method and reverse-transcribed into complementary DNA (cDNA) using the RevertAid First Strand cDNA Synthesis Kit (K1621, Fermenta Biotech Company). The cDNA products were amplified by PCR using the common primers pcDNA3.1-F at the 5´ end and pcDNA3.1-R at the 3´ end and analyzed by 1.5% agarose gel electrophoresis.

Plasmid construction and immunofluorescence

The *EYA1* cDNA full-length fragment and the fragment missing exon 11 were obtained by gene synthesis. The PCR products and the pLVX-flag vector were digested with the restriction enzymes Not I and EcoR I and ligated into the same restriction sites to generate the recombinant overexpression plasmids pLVX-flag-*EYA1*-WT/Mut. The plasmid pcDNA3.1-SIX1 was purchased from Youbio Biotech Company. Next, 293T cells were transiently transfected with the pLVX-flag-*EYA1*-WT/Mut plasmids and cultured in DMEM/high glucose containing 10% FBS at 37 °C with 5% CO_2. Transfected 293T cells were seeded on 24-mm coverslips in a 6-well plate at 37 °C overnight. Cells were fixed with 4% paraformaldehyde for 30 minutes, permeabilized with 1% Triton X-100 for 20 minutes, blocked using 5% bovine serum albumin for 30 minutes at room temperature, and further incubated with a primary antibody against Flag (Abmart Cat# M20008, RRID: AB_2713960) at 4 °C overnight. On day 2, the cells were incubated with secondary antibodies for 1 hour at room temperature, followed by incubation with DAPI to visualize the cell nucleus.

Immunoprecipitation

We cotransfected the plasmids pLVX-Flag-vector and pLVX-Flag-EYA1-WT/Mut with pcDNA3.1-SIX1 into 293T cells. The transfected 293T cells were lysed in immunoprecipitation (IP) lysis buffer (P70100, NCM Biotech) containing protease inhibitor and phosphatase inhibitor cocktail 1/2, and the supernatant was collected after centrifugation for IP. After the detection of protein concentration, a portion of the protein was taken out for input, and the remaining 6,000 μg protein was used for IP. Cell lysates were incubated with anti-FLAG M2 magnetic beads (M8823, Sigma-Aldrich) at 4 °C overnight. The beads were equilibrated with Tris-buffered saline (TBS; 50 mM Tris HCL, 150 mM NaCl, pH 7.4) in advance. Then, the beads were captured using a magnetic stand and washed with TBS three times. Subsequently, 50 μL of 100 ng/μL of 1X FLAG peptide (F3290, Sigma-Aldrich) solution was added to the magnetic beads and incubated for 30 minutes at room temperature on an orbital shaker to acquire the precipitated proteins.

Cycloheximide treatment

Next, 293T cells were transiently transfected with the pLVX-flag-*EYA1*-WT/Mut plasmids and cultured in DMEM/high glucose containing 10% FBS at 37 °C with 5% CO_2. Cycloheximide (C7698, Sigma-Aldrich) at a final concentration of 50 μg/mL was added to the medium to stop protein synthesis at the indicated time before Western blotting analysis.

RESULTS

Clinical characteristics

We collected a BOS pedigree containing four patients in three consecutive generations (Fig. 1A) and performed a detailed clinical examination and genetic analysis according to the criteria proposed by Chang et al. [12]. The clinical characteristics are shown in Table 1. Proband III-1 and patient III-2 were 15-year-old twin brothers with similar physical characteristics, presenting with bilateral mild to moderate conductive HL and preauricular pits. Patients I-1 and II-2 both presented with bilateral moderate to profound mixed HL and preauricular pits, while patient II-2 presented with right earlobe agenesis (Fig. 1C). Branchial fistulas occurred bilaterally in patients I-1 and III-1 and unilaterally in patients II-2 and III-2. All patients lacked renal anomalies based on examinations of urinary system function and urological ultrasonography. Facial asymmetry was observed in patients

Table 1. Clinical characteristics of the BOS patients in this study

Patient	Sex	Age (yr)	HL type	Preauricular pits	Branchial fistulae	Renal anomalies	Other BOS symptom	Nucleotide change
I 1	M	60	+, Mixed HL, b	+, b	+, b	–	Facial asymmetry	*EYA1* C.1050+4 A>C
II 2	F	37	+, Mixed HL, b	+, b	+, un	–	Facial asymmetry, external ear anomaly (R)	*EYA1* C.1050+4 A>C
III 1	M	15	+, Conductive HL, b	+, b	+, b	–	Ossicular chain malformation	*EYA1* C.1050+4 A>C
III 2	M	15	+, Conductive HL, b	+, b	+, un	–	Ossicular chain malformation	*EYA1* C.1050+4 A>C

The symbol "+" indicates a positive symptom; the symbol "–" indicates the absence of a clinical symptom.
BOS, branchio-oto syndrome; HL, hearing loss; b, bilateral; un, unilateral.

III-1 and II-2, but not in patients III-1 and III-2. We further evaluated the structure of the middle and inner ear in patients III-1 and III-2 using high-resolution computed tomography (HRCT) of the temporal bone, and both patients showed malformations of the ossicular chain (data not shown), which were consistent with their auditory test results. All affected members within the family exhibited some degree of clinical heterogeneity in HL and branchial fistulas, as well as other symptoms such as external and middle-ear anomalies.

Clinical treatment

We performed surgery on the affected right ear of the proband (Fig. 2A) and observed that the incus was malformed and that the long process of the incus was shortened, forming a loosened pseudo-junction with the stapes head involving only soft tissue, which affected the conduction efficiency of the ossicular chain (Fig. 2B and C). Therefore, we performed type II tympanoplasty using a PORP artificial ossicle after removal of the deformed incus. The hearing of Patient III-1 significantly improved after surgery, and the follow-up PTA data showed a reduction in the airbone gap (Fig. 2D and E).

Genetic analysis

To further explore the causative genes, we performed WES on the affected members (I-1 and III-1) and an unaffected person (III-3) within the family. After essential quality control and assessment of the sequenced data, the variants that were predicted to be harmful or affect alternative splicing according to prediction software such as combined annotation dependent depletion (CADD) and dbscSNV were retained [23,24]. In general, a coverage depth of the targeted region of at least 20-fold was considered to indicate reliability, and the mean sequencing depth was 100-fold. Then, we investigated all known causative genes (*EYA1, SIX1, SIX5*) associated with BOS and identified a novel candidate variant, c.1050+4 A>C, in the *EYA1* gene (Fig. 1B). Detailed information on the novel variant, including population data and *in silico* data, can be found in Supplementary Table 1. The evaluation of the variant evidence was categorized separately according to the American College of Medical Genetics and Genomics guidelines (PM2, PP1) and the Clinical Genome Resource (ClinGen) Sequence Variant Interpretation (SVI) Working Group recommendations (PVS1(RNA)) [25,26]. The novel splicing variant was classified as pathogenic.

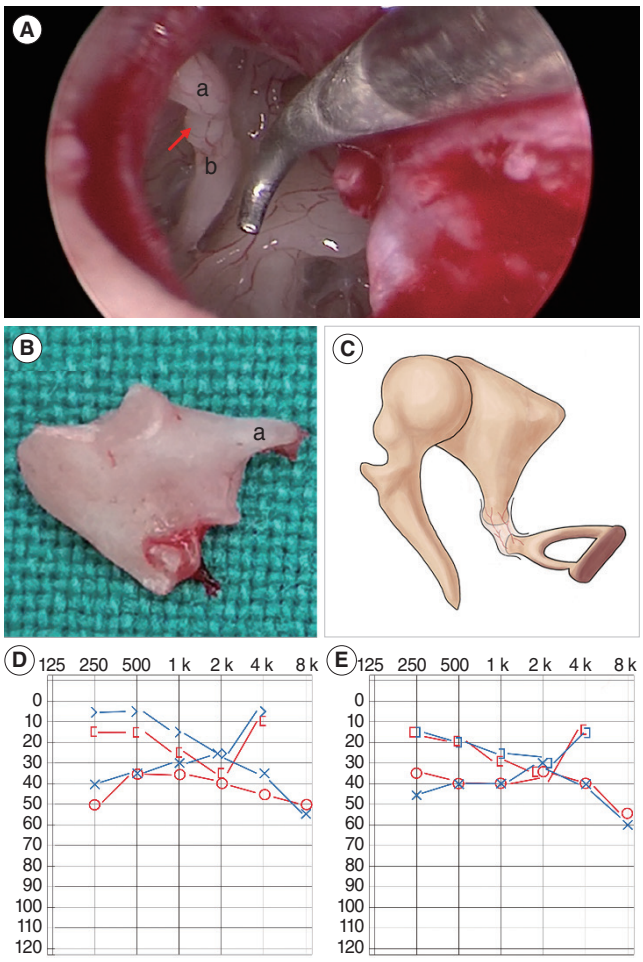

Fig. 2. The surgical treatment and postoperative effect of the proband. (A) The visual field of the middle ear operation cavity of the proband. The position marked by "a" represents the long process of the incus, and "b" represents the stapes head. The red arrow indicates the loosened pseudo-junction at the incudostapedial joint position. (B, C) The dysplastic incus is shown in B, and a schematic diagram of its participation in the formation of abnormal ossicular chains is shown in C. (D, E) Audiograms of the proband at 1 month and 6 months after middle-ear surgery.

Sanger sequencing was performed to verify that the patients carried the candidate variant and the unaffected individuals did not for the cosegregation test (Fig. 1B). The *EYA1* c.1050+4 A>C

Table 2. Summary of splice-region variants in EYA1 registered in HGMD and DVD (2023.04)

Location (exon/IVS)	Nucleotide change	ACMG classification	Phenotype (B, D, P, R)	CADD Phred	Severity of HL	FH	HL type	Ethnicity	Database	Study
Exon 6	c.418 G>A	Pathogenic	B, D, P	33	Mild-profound	S	C, M	Korean	DVD	Kim et al. (2014) [5]
IVS 6	c.418+1 G>C	Pathogenic	B, D, R	34	NA	S	S	Japanese	HGMD, DVD	Unzaki et al. (2018) [3]
IVS 7	c.557-2 A>G	Pathogenic	B, P, D	34	Moderate	NA	C	Canadians	HGMD, DVD	Stockley et al. (2009) [27]
Exon 8	c.638 A>T	Pathogenic	B, D, P, R	33	NA	S	NA	American	DVD	Orten et al. (2008) [28]
Exon 8	c.639 G>C	Pathogenic	NA	36	NA	NA	NA	American	DVD	Orten et al. (2008) [28]
IVS 8	c.639+1 G>C	Pathogenic	B, D, P	34	NA	F	NA	American	HGMD, DVD	Orten et al. (2008) [28]
IVS 8	c.639+2 delA	Pathogenic	B, D, P	32	NA	F	NA	American	HGMD, DVD	Orten et al. (2008) [28]
IVS 8	c.640-15 G>A	Pathogenic	B, D, P, R	22.8	NA	F	NA	American	HGMD	Orten et al. (2008) [28]
Exon 9+IVS 8	c.640-15_698 del GAGC…AACC	Pathogenic	NA	NA	NA	F	NA	American	DVD	Vervoort et al. (2002) [29]
Exon9	c.826 G>T	Pathogenic	D (1/3), P (2/3), R (1/3)	62	NA	F	NA	American	DVD	Clarke et al. (2006) [30]
Exon 10	c.965 A>G	Pathogenic	D (4/4), P (4/4), R (NA)	33	Severe	F	M	Korean	DVD	Song et al. (2013) [11]
IVS 10	c.966+1 G>C	Pathogenic	B, D	34	NA	S	NA	American	DVD	Mann et al. (2019) [31]
IVS 10	c.966+5 G>A	Pathogenic	B (2/3), D (3/3), P (2/3), R (3/3)	18.45	Mild-moderate	F	M	Canadians	HGMD, DVD	Stockley et al. (2009) [27]
IVS 10	c.966_966+14 del TGGCTATGACGTACC	Pathogenic	B, D, P	32	NA	S	NA	French	DVD	Krug et al. (2011) [32]
IVS 10	c.967-2 A>G	Pathogenic	B (3/4), D (3/4), P (4/4)	34	Mild-moderate	F	M	Korean	HGMD, DVD	Kwon et al. (2009) [33]
IVS 10	c.967-2 A>G	Pathogenic	B (3/3), D (3/3), P (3/3)	34	Profound	F	M	Chinese	DVD	Chen et al. (2019) [34]
IVS 10	c.967-1 G>A	Pathogenic	B, D, R	35	NA	F	NA	British	HGMD, DVD	Rickard et al. (2000) [35]
Exon 11	c.967 A>T	Pathogenic	B (3/6), D (6/6), P (5/6), R (1/6)	41	NA	F	C, M	Chinese	DVD	Wang et al. (2018) [36]
IVS 11	c.1050+1 G>C	Pathogenic	B (5/5), D (5/5), P (5/5), R (1/5)	35	Mild	F	C, M	Danes	HGMD, DVD	Henriksen et al. (2004) [37]
IVS 11	c.1050+1 G>T	Pathogenic	B, D, P, R	35	NA	F	NA	American	HGMD, DVD	Orten et al. (2008) [28]
IVS 11	c.1050+1 G>T	Pathogenic	B (1/2), D (2/2), P (2/2)	35	Moderate-profound	F	M	Chinese	HGMD, DVD	Feng et al. (2021) [17]
Exon 11+IVS 11	c.1048_1050+1 delCCCT	Pathogenic	B, D, P, R	37	NA	F	NA	American	DVD	Orten et al. (2008) [28]
IVS 11	c.1050+2 T>C	Pathogenic	D, P, R	33	NA	S	NA	Japanese	HGMD, DVD	Unzaki et al. (2018) [3]
IVS 11	c.1050+4 A>C	Pathogenic	B (4/4), D (4/4), P (4/4)	17.23	Moderate-profound	F	C, M	Chinese	-	This study
IVS 11	c.1051-12 T>G	Pathogenic	B, D, P	25.7	NA	F	NA	American	HGMD	Orten et al. (2008) [28]
IVS 11	c.1051-2 A>G	Pathogenic	B (2/3), D (3/3), P (3/3), R (1/3)	34	NA	F	NA	Japanese	HGMD, DVD	Okada et al. (2006) [38]
IVS 11	c.1051-1 G>C	Pathogenic	B, D, P	34	NA	F	NA	American	HGMD, DVD	Orten et al. (2008) [28]
Exon12	c.1051 G>T	Pathogenic	B (1/3), D (3/3), P (3/3), R (1/3)	35	NA	F	NA	Japanese	DVD	Okada et al. (2006) [38]
Exon12	c.1138 G>T	Pathogenic	B (1/2), D (1/2), P (2/2)	46	NA	F	NA	French	DVD	Krug et al. (2011) [32]
Exon 12+IVS 12	c.1138_1140+1 delinv GAAG	Pathogenic	B , D, P	33	NA	F	NA	American	DVD	Orten et al. (2008) [28]
IVS 12	c.1140+1 G>A	Pathogenic	B, D, P	34	Moderate-profound	S	M	Chinese	HGMD, DVD	Feng et al. (2021) [17]

(*Continued to the next page*)

Table 2. Continued

Location (exon/IVS)	Nucleotide change	ACMG classification	Phenotype (B, D, P, R)	CADD Phred	Severity of HL	FH	HL type	Ethnicity	Database	Study
IVS 12	c.1140+1 G>A	Pathogenic	D, P, R (NA)	34	Moderate	S	M	Korea	HGMD, DVD	Song et al. (2013) [11]
IVS 12	c.1140+1 G>T	Pathogenic	B, D, R	35	NA	F	NA	British	HGMD, DVD	Rickard et al. (2000) [35]
IVS 12	c.1141-1 G>A	Pathogenic	B (12/14), D (17/18), P (9/9), R (3/7)	35	Mild-severe	F	C, M, S	British	HGMD, DVD	Sanggaard et al. (2007) [39]
IVS 13	c.1199+1 G>C	Pathogenic	B, D, P, R	34	NA	S	NA	French	HGMD, DVD	Krug et al. (2011) [32]
IVS 14	c.1360+4 A>G	Pathogenic	B (19/21), D (21/21), P (18/21), R (4/7)	22.9	NA	F	M	British	HGMD, DVD	Sanggaard et al. (2007) [39]
IVS 14	c.1360+5 G>A	Pathogenic	B, D, R	22.6	Moderate-profound	S	C	Canadians	HGMD, DVD	Stockley et al. (2009) [27]
Exon 15	c.1475 G>C	Pathogenic	NA	36	NA	F	NA	American	DVD	Orten et al. (2008) [28]
Exon 15	c.1471_1474 dupGGGA	Pathogenic	B (2/2), D (2/2), P (2/2), R (2/2)	33	NA	F	NA	French	DVD	Krug et al. (2011) [32]
Exon15	c.1474 dupG	Pathogenic	B (3/3), D (3/3), R (2/3)	36	Severe	F	S	Korean	DVD	Kim et al. (2005) [40]
IVS 15	c.1475+1 G>C	Pathogenic	B, D, P, R	34	NA	S	C	Italians	HGMD, DVD	Gigante et al. (2013) [41]
IVS 15	c.1476-2 A>G	Pathogenic	B, D, P, R	33	NA	F	NA	American	HGMD	Orten et al. (2008) [28]
Eon 16	c.1597 G>A	Pathogenic	B, D ,P	35	Mild	S	C	Italians	DVD	Castiglione et al. (2014) [42]
IVS 16	c.1597+2 T>G	Pathogenic	NA	34	NA	S	NA	French	HGMD, DVD	Abdelhak et al. (1997) [43]
IVS 16	c.1598-2 A>C	Pathogenic	B, D, P	33	Moderate-profound	S	M	Korean	HGMD, DVD	Song et al. (2013) [11]
IVS 16	c.1598-1 G>A	Pathogenic	B, D, P, R	34	NA	S	NA	Japanese	HGMD, DVD	Okada et al. (2006) [38]
Exon 17	c.1697 dupA	Pathogenic	B, D, P, R	36	NA	F	NA	American	DVD	Orten et al. (2008) [28]
Exon 17	c.1695_1698 delCTTT	Pathogenic	B (7/8), D (8/8), P (7/8), R (3/8)	39	NA	F	NA	Netherlander	DVD	Kumar et al. (1998) [44]
IVS 17	c.1698+1 G>A	Pathogenic	B (2/2), D (2/2), P (2/2), R (2/2)	34	NA	F	NA	Spanish	HGMD, DVD	Rodriguez-Soriano et al. (2001) [45]
IVS 17	c.1698+1 G>T	Pathogenic	B, D, P	35	NA	F	NA	American	HGMD, DVD	Orten et al. (2008) [28]
IVS 17	c.1698+5 G>C	Pathogenic	NA	21	NA	S	NA	French	HGMD, DVD	Abdelhak et al. (1997) [43]

The genetic spectrum of *EYA1* pathogenic mutations in the splicing region. *EYA1* canonical transcript NM_000503.6. For the phenotype column, the numerator represents the count of patients exhibiting the corresponding phenotype, and the denominator represents the total number of branchio-oto syndrome/branchio-oto-renal syndrome within the family.

HGMD, Human Gene Mutation Database; DVD, Deafness Variation Database; IVS, intervening sequence; ACMG, American College of Medical Genetics and Genomics; B, branchial anomalies; D, deafness; P, preauricular fistulae; R, renal anomalies; CADD, combined annotation dependent depletion; FH, family history; S, single patient; NA, not available; F, family; HL, hearing loss; C, conductive HL; M, mixed HL; SHL, sensorineural HL.

variant in the proband was confirmed to be derived from the affected grandfather. *EYA1* c.1050+4 A>C is a novel splicing variant located in the splicing donor site of exon 11 and has not been recorded in public databases, including gnomAD and ClinVar. Although the variant at position +4 is not located at a canonical splice site, such as the –1, –2, +1, and +2 residues around the exon–intron junction, the predicted splicing effect of c.1050+4 A>C, generated by SpliceAI, suggests that causes donor loss of exon 11 and aberrant splicing of the EYA1 transcript [46,47]. As the most common causative gene in 40% of patients with BOS and BORS, many variation types have been identified in *EYA1*, among which frameshift and splicing mutations predominate [10,17]. We have summarized the 48 pathogenic variants of the *EYA1* gene in the splice region (Fig. 3A), including the canonical and noncanonical splice sites, from The Human Gene Mutation Database (HGMD, public site version) and Deafness Variation Database (DVD), as well as this study (Table 2). Pathogenic canonical and noncanonical splice sites of the *EYA1* gene account for 73% (35/48) and 27% (13/48) of the variants in the splice region, respectively, and are mainly located in the ED of EYA1. A conservation analysis of the amino acid sequence of exon 11 was performed between humans and other vertebrate animal species and showed that the fragment is highly conserved across species (Fig. 3B). The reference transcript and protein sequences of *EYA1* in this study were NM_000503.6 and NP_000494.2, respectively.

Minigene and 3D protein modelling assays

Although *EYA1* c.1050+4A>C is a noncanonical splicing variant, given the deleterious inferences from several pathogenicity prediction software programs, we decided to verify the potential aberrant splicing by a minigene assay, which simulates the *in vivo* splicing process [48]. The two successfully constructed pcMINI-*EYA1*-WT/Mut plasmids were transfected into HeLa and 293T cells separately for 48–72 hours (Fig. 4A). The total RNA was then extracted from the transfected cells and reverse-transcribed into cDNA. The target region, exon 11 of *EYA1*, was amplified by PCR, and the product band was analyzed by agarose gel electrophoresis. Two bands of the mutant type and one band of the wild type were observed by agarose gel electrophoresis and named bands A and B, respectively (Fig. 4B). Band A was the same size in the mutant type and the wild type, but the mutant exhibited a lower band B, indicating a partial deletion of the target region. In addition, band B was much brighter than band A in the mutant. We performed a greyscale analysis of each band using ImageJ software to calculate the number of each transcript from the wild type and mutant. The results showed that the expression of band A in the mutant was reduced by approximately 60% versus the wild type (Fig. 4B). The Sanger sequencing results also confirmed that only an aberrant pre-mRNA product was found in the mutant. Compared with the reference transcript, after sequencing and aligning bands A and B, it was found that band A retained the complete sequence, while band B lacked the entire exon 11 sequence, which had a length of 84 bp (Fig. 4C and D).

Given the findings of the aberrant splicing model, we resolved the crystal structure of the EYA1 protein (referred to as called EYA1-WT) by AlphaFold v2.0 software, and we attempted to analyze where exon 11 was found in the protein space conformation of EYA1 and possible functional impairment of the mu-

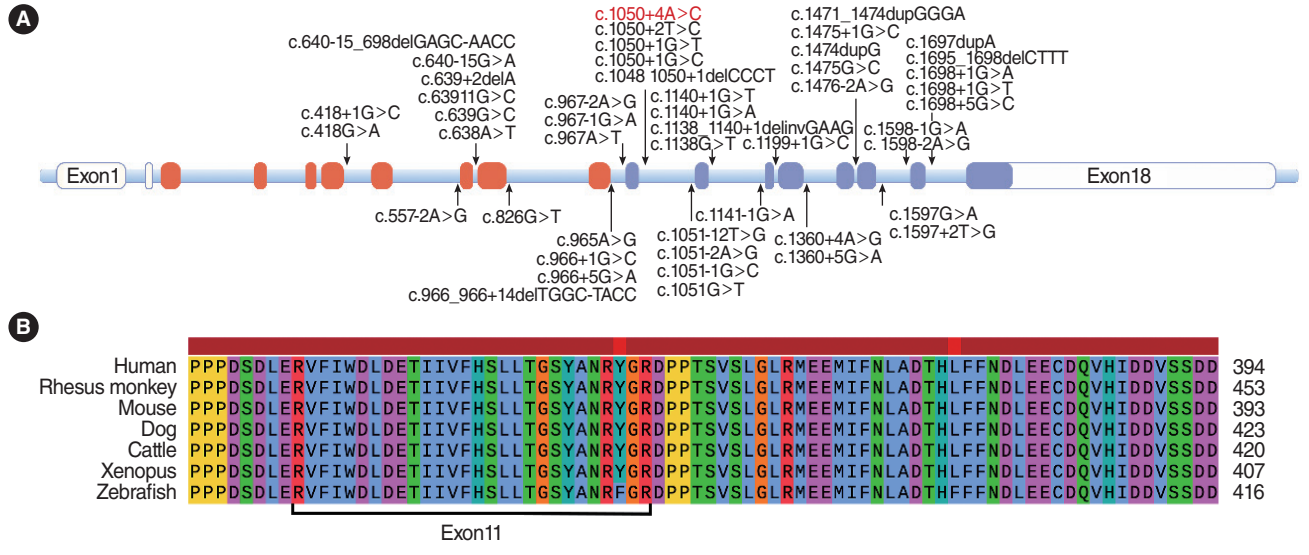

Fig. 3. Mutational spectrum of the *EYA1* splicing region associated with Branchio-oto syndrome/branchio-oto-renal syndrome and conservation analysis. (A) The 18 exons of *EYA1* are arranged in an oval shape, starting with exon 1. The orange oval represents the divergent transactivated domain at the N-terminus, and the blue oval represents the highly conserved EYA domain (ED) at the C-terminus. There are 48 pathogenic variants in the splicing region, mainly in the ED. The novel mutation in this study is marked in red. (B) The amino acid sequence encoded by exon 11 of the *EYA1* gene is a highly conserved region among different species.

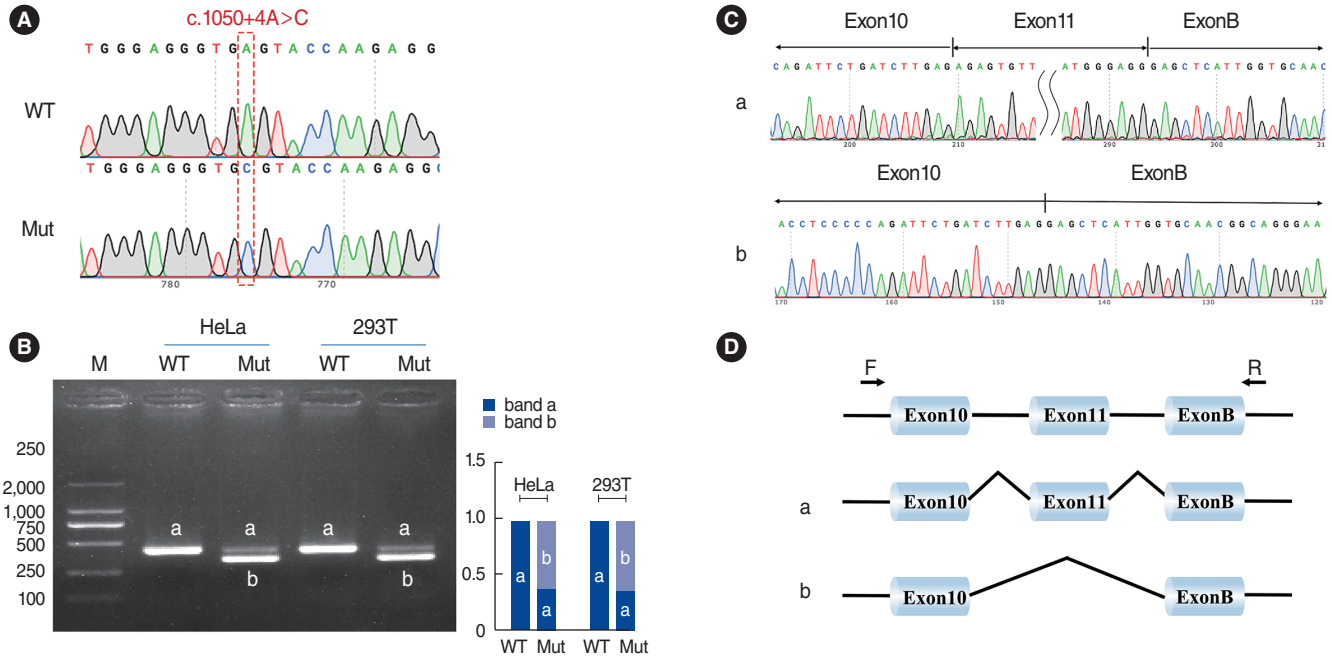

Fig. 4. Aberrant pre-mRNA splicing was identified by minigene assay. (A) The Sanger sequencing results showed that both wild-type (WT) and mutant (Mut) minigene plasmids were successfully constructed. (B) The upper band a corresponds to the normal pre-mRNA, and the lower band b corresponds to the aberrant pre-mRNA. The quantitative analysis of the bands (right). (C) The sequencing result of band b with exon 11 skipping. (D) The schematic diagram presents the target region of the above sequencing and indicates that the c.1050+4 A>C splicing mutation could lead to the skipping of the entire exon 11 of *EYA1* pre-mRNA. F, Forward; R, Reverse.

tated protein (EYA1-Mut) by exon 11 skipping. The protein structure covering the sequence from residues Ser-319 to Leu-592 was characterized by a high level of confidence and consisted mainly of the highly conserved ED region (Arg323-Leu592), as shown in Fig. 5A and B. The protein structure encoded by exon 11 is marked in green (Fig. 5A). The crystal structure of the EYA1-Mut protein not only lacked the secondary structures of alpha helix 1 (α1), alpha helix 2 (α2) and beta-sheet 1 (β1), which are encoded by exon 11, but also exhibited damage to the structure of the beta-sheet 2 (β2) and beta-sheet 4 (β4) motif compared with EYA1-WT (Fig. 5B). Protein–protein docking not only facilitates the analysis of the EYA1-SIX1 interface, but also assists in elucidating the potential damage to EYA1-SIX1 protein interactions caused by the deletion of the exon 11 section of the EYA1 protein. The interface area of EYA1-WT with SIX1 protein was 932.5 Å^2, while that of EYA1-Mut was reduced to 844.4 Å^2. With the absence of exon 11, the residues Glu322, Asn494, and Lys548, as well as the β2 motif, which were originally located at the EYA1-SIX1 protein interface, do not participate in the formation of the contact interface (Fig. 5C and D).

Immunofluorescence and protein expression

As established in the genetic diagnosis, we determined at the genome level that the splicing variant *EYA1* c.1050+4 A>G leads to exon 11 skipping of *EYA1* mRNA at the transcriptome level, which in turn could potentially affect EYA1 protein expression and function. We further constructed pLVX-Flag-*EYA1*-WT/Mut plasmids to investigate the subcellular distribution of EYA1-WT/Mut proteins in 293T cells. The immunofluorescence results showed that the overexpressed intact EYA1 protein was dispersed in both the cytoplasm and nucleus, while the defective EYA1 protein was distributed only in the cytoplasm (Fig. 6B). The results of the nucleoplasm separation experiment confirmed this finding. The protein expression of EYA1-WT and EYA1-Mut was assessed in 293T cells transfected with the overexpressed wild-type and mutant plasmids. The results suggested that the EYA1-Mut protein was reduced compared to the wild type (Fig. 6A).

Nucleoplasm separation analysis

Nuclear cytoplasmic separation was performed on 293T cells cotransfected with the plasmids pLVX-Flag-EYA1-WT/Mut and pcDNA3.1-SIX1, and the results showed that the EYA1 mutant protein had no detectable expression in the nucleus (Fig. 6C). By interacting with the wild-type SIX1 protein derived from cotransfection with the pcDNA3.1-SIX1 plasmid, the wild-type EYA1 protein could be aggregated in the nucleus, whereas this was not possible for the defective EYA1 protein.

Immunoprecipitation analysis

An IP assay was performed to investigate the functional defects of the defective EYA1 protein. We explored the EYA1-SIX1 interactions in EYA1-WT and EYA1-Mut in 293T cells by cotransfection with the plasmids pLVX-Flag-EYA1-WT/Mut and pcDNA3.1-SIX1. The protein loading amount of the input group was the

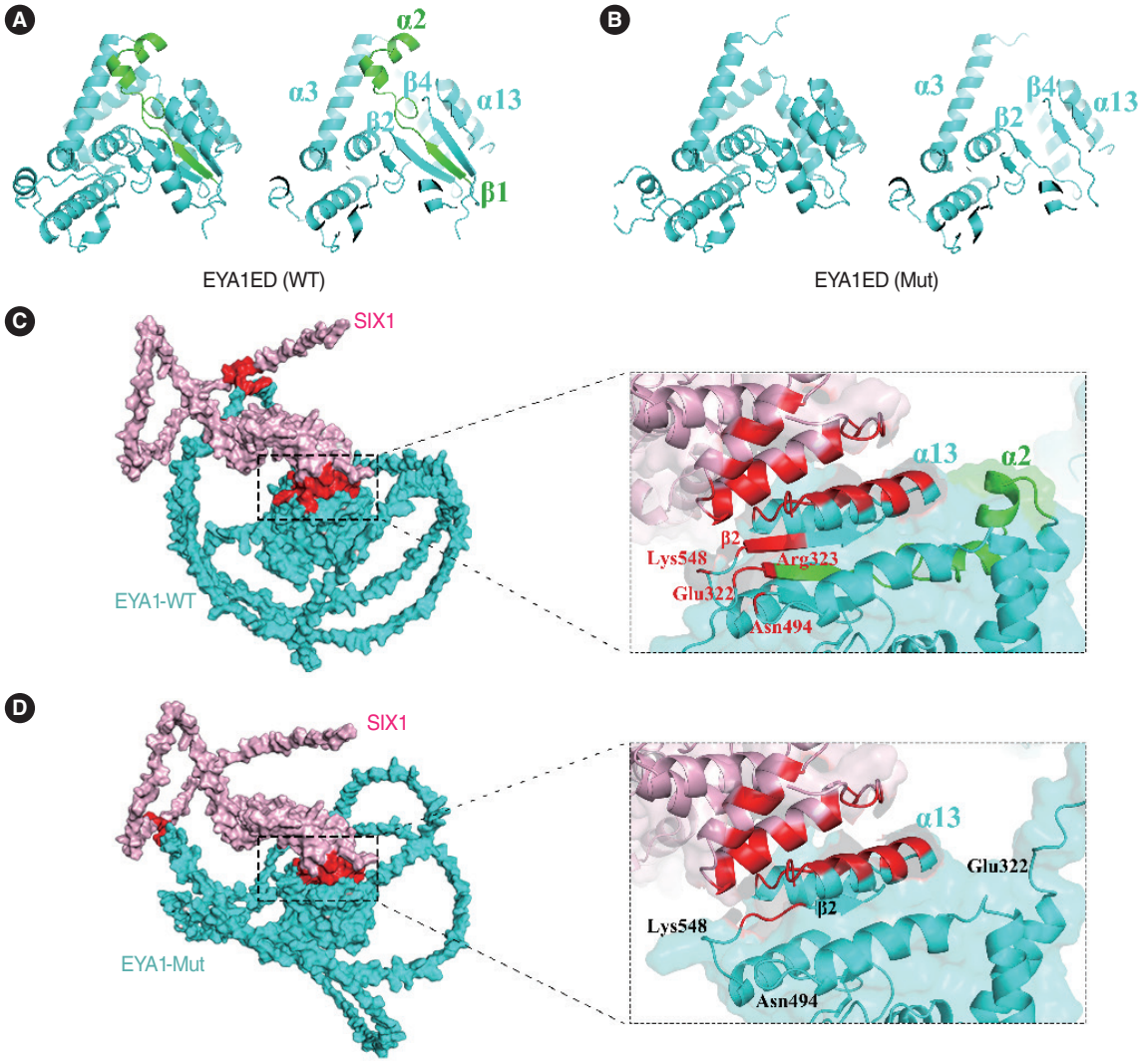

Fig. 5. Crystal structure prediction. (A, B) The EYA domain (ED) structure of EYA1-WT and EYA-Mut. The front (left) and internal (right) views of the overall protein structure. The exon 11 section is marked in green. (C, D) Prediction of protein–protein docking between EYA1-SIX1, with the interface area marked in red. The enlarged images in the dotted box show the amino acid residues and structure that were originally located at the protein-protein interface and later changed. α, alpha helix; β, beta sheet.

same; however, in order to quantitatively detect the binding amount of SIX1 in the IP group, Flag-EYA1 protein levels in EYA1-WT and EYA1-Mut were aligned to detect differences in the EYA1-SIX1 interactions. The EYA1-Mut protein did not pull down the SIX1 protein (Fig. 6D).

The EYA1-Mut protein is less stable than EYA1-WT

To assess the stability of the EYA1-WT and EVA1-Mut proteins, we treated transfected 293T cells with cycloheximide (50 μg/mL) at specific times. Western blotting was then performed to detect the protein levels of EYA1-WT/Mut after cycloheximide treatment. As expected, the stability of the EYA1-Mut protein was considerably reduced. Additionally, the experiment also showed that the half-life of the EYA1-Mut protein was shorter than that of EYA1-WT (Fig. 6E).

DISCUSSION

In this study, we characterized the clinical phenotypes and performed a genetic analysis in a Chinese family with BOS. Clinical treatment of auditory reconstruction was performed for the proband, and his hearing significantly improved. The novel splicing variant *EYA1* c.1050+4 A>C was identified, which causes aberrant splicing and leads to the abnormal distribution and attenuation of the *EYA1* mutant protein, further supplementing the mutational spectrum of BOS/BORS-related genes. We systematically explored the pathogenicity and molecular mechanisms of *EYA1* c.1050+4 A>C.

The regional distribution of BOS/BORS patients is mainly concentrated in developed countries such as Denmark, Canada, Korea, Japan, and the USA, and it has been rarely reported in

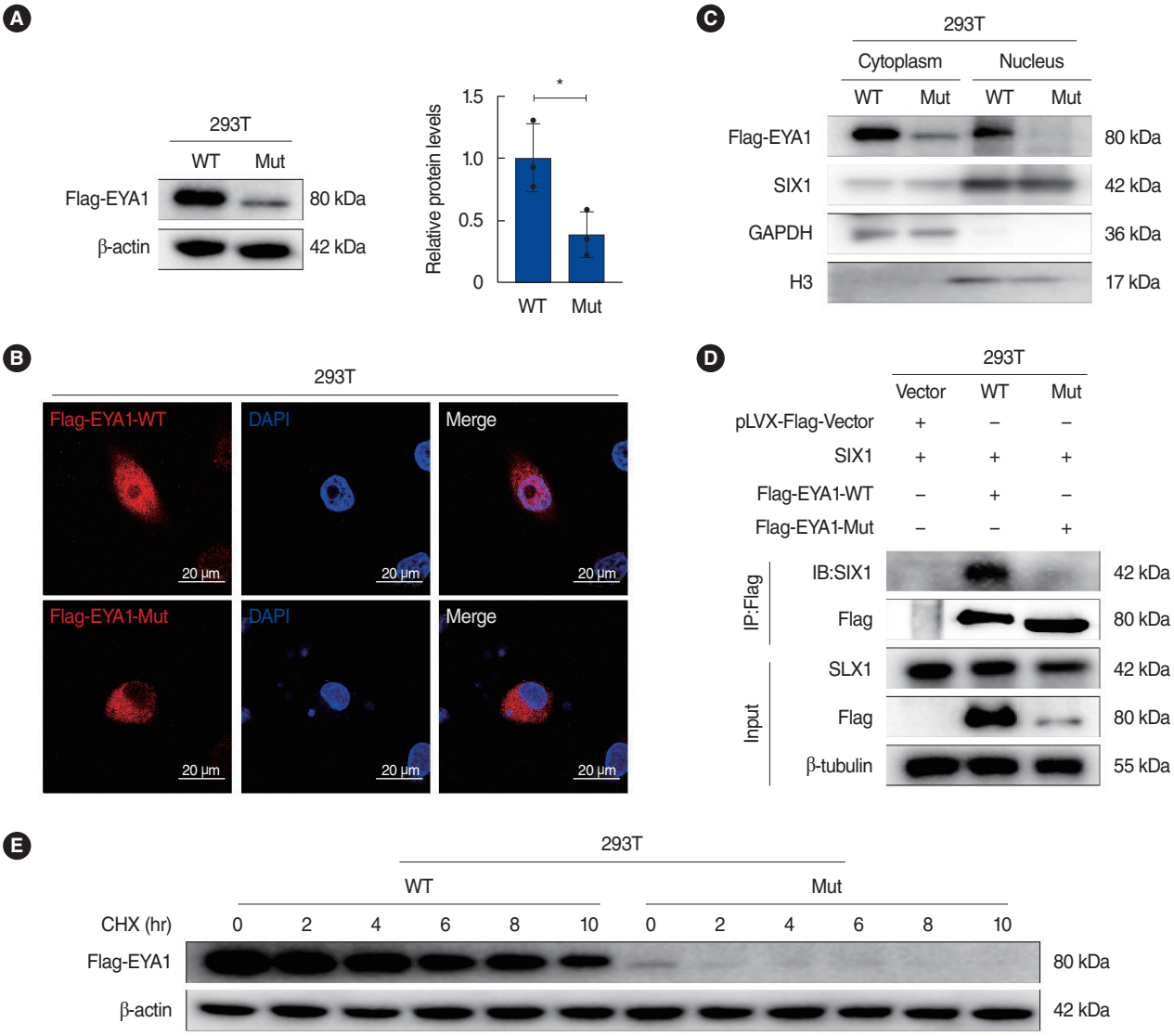

Fig. 6. Abnormal function of the EYA1 mutant protein. (A) Decreased expression of the EYA1 mutant protein. The error bars indicate standard deviation. *P<0.05, calculated using the t-test in Prismr9. (B) Cellular sublocalization of EYA1 wild-type and defective proteins. (C) Nucleoplasm separation further verified that the defective EYA1 protein failed to enter the nucleus. (D) Lysates from 293T cells transiently overexpressing the vector and EYA1-WT/MUT with Flag were subjected to immunoprecipitation assays. (E) The decay kinetics of the EYA1-WT and EYA1-MUT proteins using cycloheximide (CHX). The experiment was repeated three times, and a representative result is shown. WT, wild-type; Mut, mutant; GAPDH, glyceraldehyde-3-phosphate dehydrogenase; DAPI, 4´,6-diamidino-2-phenylindole.

China [10]. Recent reports of BOS/BORS in the Chinese population have gradually increased, which could be attributed to increased clinical attention and the development of high-throughput sequencing technology. Feng et al. [17] concluded that BOS is the primary pattern in Chinese patients as opposed to patients from other Asian countries, as patients with renal anomalies account for only 13.88%. None of the patients in their study showed abnormalities in examinations of the urinary system.

BOS/BORS is a group of syndromic deafness disorders that exhibit wide interfamilial and intrafamilial phenotypic variability [3,49]. In the present study, patients with BOS within the family carrying the same causative variant presented both conductive and mixed HL types. In addition, branchial fistulas were not always observed bilaterally. As the predominant symptom, HL has been reported in nearly 98% of affected BOS/BORS patients, varying from mild to profound, with nearly half of patients expressing a mixed type, followed by the conductive and sensorineural types [11,12,50]. In addition to the primary BOS symptoms described above, the other observed minor symptoms, such as facial asymmetry and earlobe agenesis, were absent in every patient. The genotype-phenotype correlations of BOS/BORS have not yet been fully defined. The existence of interfamilial phenotypic variability has also been proven. A patient from the United States with the causative mutation c.1050+1 G>T of *EYA1* ex-

hibited renal anomalies. However, patients from China with the same causative mutation did not exhibit such anomalies (Table 2). Genotypic heterogeneity is also present in BOS/BORS. The distinct variants c.967-2 A>G and c.1050+4 A>C of *EYA1* caused similar major symptoms of BOS in all individuals of two unrelated families, as well as a similar type and severity of HL.

The *EYA1* c.1050+4 A>C mutant protein was distributed in the cytoplasm, and the protein expression level decreased (Fig. 6A-C). As a critical genetic risk factor, the *EYA1*-encoded protein is broadly expressed across the embryonic to postnatal stages and is involved in regulating mammalian cranial neural crest cell differentiation; it consists of a highly conserved ED containing 271 amino acids at the C-terminus and a divergent N-terminal transactivated domain [51-54]. The ED amino acid sequence is highly conserved across species via interaction with the SIX domain (SD) of the SIX1 protein to achieve intranuclear translocation of the EYA1 protein and further utilize its transcriptional activity to regulate organogenesis [55,56].

An Eya1-deficient mutant mouse model exhibits multiple morphological deformities of the inner, middle, and outer ear resembling BOS/BORS. The middle ear ossicles originate from the cranial neural crest cells located in the first and second branchial arches [57]. Eya1-mutant mice have abnormal branchial arch morphology development and ossicle anomalies, such as a deformed structure in the incudomalleolar joint [58]. These findings from animal studies may explain why the proband developed malformations and functional abnormalities of the middle ear ossicles.

The transient minigene experiment is a common approach for identifying potential aberrant pre-mRNA splicing caused by mutations in the splicing region *in vitro* [56]. Approximately 95% of the pre-mRNA of eukaryotic genes undergoes alternative splicing events, resulting in highly diverse transcripts and protein products, which play an essential role in multiple hereditary diseases [59]. Abnormal regulation of alternative splicing of pre-mRNA may produce transcripts and proteins with different or opposite functions from the conventional homologous products, thereby causing diseases. Several *in silico* prediction methods are currently more and more accurate in predicting the harmfulness of canonical splicing mutations. However, these methods' sensitivity and specificity for noncanonical splicing mutations still require improvement. A minigene experiment can simulate the effect of a splicing mutation *in vitro*. The results of the minigene assay demonstrated that the A>C point mutation at the +4 position could lead to the skipping of the entire exon 11 of *EYA1* pre-mRNA, may impair the EYA1-SIX1 protein interaction due to aberrant RNA splicing, and may be involved in disease occurrence.

In the predicted crystal structure model of the EYA1 protein and protein–protein docking at the EYA-SIX1 interface. The tertiary structure of defective EYA1 proteins was altered, and the interface area decreased, which may affect the structural stability of the protein itself and further reduce the binding level of EYA1-SIX1 interactions. The protein-protein interface is the region where two protein chains interact and form an array of polar and nonpolar contact, involving hydrophobic interactions [60,61]. Interactions between protein molecules rely on surface complementarity, including the spatial structural complementarity of the shape matching of the contact surfaces, and the complementarity of the physical and chemical properties of the weak bonds that bring the complex together [62,63]. As the absence of exon 11 leads to changes in the spatial structure of the mutant protein, the amino acid residues Glu322, Asn494, and Lys548 that were originally located at the EYA1-SIX1 protein interface might be exposed on the surface of the molecule, potentially decreasing the stability of protein-protein interactions. The amino acid residues Glu322 and Lys548 are polar, with negative and positive charges, respectively, and may contribute to the stabilization of EYA1-SIX1 protein spatial structure as well as biological functions by electrostatic interactions. In contrast, the nonpolar amino acid residue Asn494 might be involved in hydrophobic interactions at the EYA1-SIX1 protein interface. Interestingly, two cases of pathogenic mutations at amino acid residues Glu322 [11] and Lys548 [28] of the EYA1 protein have been reported, confirming the importance of these amino acid positions. The highly conserved amino acid residues encoded by exon 11 of *EYA1* are in the ED region, which binds with the SD region and plays a crucial role in promoting craniofacial development as a transactivating partner. The EYA1 ED is highly conserved within the EYA family and shares >90% sequence similarity with the ED of EYA2, and model comparisons of both domains indicate high similarity (Supplementary Fig. 1). In addition, there is a high degree of sequence conservation in the interaction regions between SIX and EYA family members from different eukaryotes, underlying the importance of these residues for the normal function of the complex [64]. Ideally, the molecular details of SIX1–EYA1 interactions could be determined using the crystal structure of the complex in human in the future. Therefore, Patrick et al. proposed that the SIX1-EYA2 ED structure may provide a basis for predicting the molecular mechanisms of EYA1 and provide a valuable model to guide future functional studies. In summary, the predicted protein structure model established in this study is instructive for exploring the pathogenicity of the EYA1 mutant. The skipping of exon 11 of *EYA1* leads to abnormal splicing changes in its pre-mRNA, which in turn may impair the function of the EYA-SIX1 complex.

To further analyze the potential loss of EYA1-SIX1 interactions, we performed an IP assay to investigate the functional defect of the defective EYA1 protein. The results showed that the defective EYA1 protein failed to pull down the SIX1 protein, thus suggesting that the defective EYA1 protein encoded by the skipping of exon 11 of *EYA1* could impair EYA1-SIX1 interactions. EYA1 functions upstream of the SIX1 protein and forms a complex to enter the nucleus. Therefore, we speculated that the

defective EYA1 protein has difficulty entering the nucleus and verified this conjecture through immunofluorescence experiments and nucleoplasm separation experiments. In short, the results of the IP, nucleoplasm separation, and immunofluorescence experiments confirmed that defective EYA1 functions abnormally and fails to interact with the SIX1 protein and enter the nucleus. In addition, the experimental results of CHX treatment showed that the EYA1-Mut protein not only exhibited poor stability, but also had a relatively short half-life, suggesting that the *EYA1* c.1050+4 A>C variant might cause disease, likely through haploinsufficiency, by affecting the interactions between the EYA1 and SIX1 proteins.

The frequency of carrying *EYA1* splicing mutations is higher in BOS/BORS patients. However, the resulting pre-mRNA splicing changes of most mutations have not been further explored. At present, the minigene assay has been reportedly used to study aberrant splicing changes in only a few splicing mutations of *EYA1* leading to the skipping of exons adjacent to the mutation site, such as c.418 G>A, c.966+5 G>A, c.1140+1 G>A and c.1598-2 A>C [5,11]. According to the DVD and HGMD, as well as this study, 48 pathogenic variations of *EYA1* in the splice region have been identified (Table 2), including 35 canonical and 13 noncanonical splicing variants. Notably, more variants occur at the splicing donor site than at the splicing acceptor site, at a ratio of approximately 1.5:1, and these variants more significantly affect the exon splicing regulatory sequence [65,66]. Therefore, we further observed that in *EYA1*, splicing variants that occurred at the 5´ splicing donor site (34/48, 71%) were more prevalent than those at the 3´ splicing acceptor site (14/48, 29%).

Unzaki et al. [3] proposed a genetic diagnosis algorithm in BOS/BORS patients and suggested focusing first on the genetic analysis of *EYA1, SIX1*, and *SIX5* due to their high incidence. With the improvement and lower price of gene sequencing technology, next-generation sequencing could be an efficient strategy for identifying causative genes for BOS/BORS.

BOS/BORS patients mainly manifest mixed and conductive HL [10], and there are various treatments to achieve hearing improvements, such as hearing aids, middle-ear surgery, or cochlear implantation. In this study, middle-ear surgery was successfully performed in the proband, and postoperative follow-up demonstrated effective improvement in hearing. During the operation, we observed a malformed incus with a shortened long process, which would have resulted in only a fibrous band of attachment around the incudostapedial joint, causing difficulties in effectively performing the function of sound transmission and cascade amplification.

Previous studies have held the view that middle ear surgery is somewhat limited in improving hearing in BOS/BORS patients, and few patients have achieved the ideal effect of auditory rehabilitation [67-69]. Song et al. [11] suggested that the occurrence of this phenomenon may be closely related to the abnormal development of the middle ear tympanic cavity, the enlarged vestibular aqueduct (EVA) of the inner ear, or the decrease in the mobility of the stapes due to the increased perilymphatic pressure in BOS/BORS patients. We carefully reviewed the temporal bone HRCT of the proband and confirmed that no EVA was found (Supplementary Fig. 2). Etiologically, the EVA is considered a pathological third window that prevents adequate energy delivery in the inner ear, even if the middle ear is properly reconstructed. In view of the latest research, Nam et al. [70] proposed that the presence of EVA in patients with BOS/BORS might be a negative indicator of poor prognosis for middle ear surgery. Although the currently available studies suggest a correlation between the presence or absence of EVA and the success rate of auditory improvement, this inference is limited by the small sample size of these studies and thus merits further exploration.

In conclusion, we identified a novel splicing variant of *EYA1* (c.1050+4 A>C) in four patients in three generations of a Chinese BOS family and helped Patient III-1 achieve successful auditory rehabilitation after middle ear surgery. This study not only expanded the genetic spectrum of *EYA1*, but also discovered a novel aberrant pre-mRNA splicing event, offering us new insights into the pathogenic mechanism of this mutation. We also collected all the variants that occurred in the splice region of *EYA1* associated with BOS/BORS to date. In addition, middle ear surgery was effective for HL in this study, suggesting that surgery can effectively improve conductive HL in BOS patients without inner ear anomalies. This finding can serve as a reference for the treatment of HL in other BOS/BORS patients.

CONFLICT OF INTEREST

No potential conflict of interest relevant to this article was reported.

ACKNOWLEDGMENTS

We thank the patients and their families who participated in this study. We are also grateful to the staff doctor of the otology department who provided the clinical treatment. We are grateful for the valuable suggestions from the reviewers.

This work was supported by the National Natural Science Foundation of China (82271187, 82071065, 82101233, 81873705), the National Key Research and Development Program Subproject (2020YFC2005204), the Hunan Province Natural Science Foundation (2021JJ41017, 2020JJ4876, 2022JJ30506), the Hunan Provincial Health Commission Program (202207014148), the University of South China Clinical Research 4310 Program, the Fundamental Research Funds for the Central Universities of Central South University (2021zzts0350).

ORCID

Anhai Chen	https://orcid.org/0000-0001-9170-457X
Jie Ling	https://orcid.org/0000-0001-7054-5119
Xin Peng	https://orcid.org/0000-0003-0601-4991
Xianlin Liu	https://orcid.org/0000-0003-3430-7353
Shuang Mao	https://orcid.org/0000-0003-0973-3393
Yongjia Chen	https://orcid.org/0000-0003-0949-9701
Mengyao Qin	https://orcid.org/0000-0002-4510-6533
Shuai Zhang	https://orcid.org/0000-0001-6314-2442
Yijiang Bai	https://orcid.org/0000-0001-8395-4595
Jian Song	https://orcid.org/0000-0002-8447-8647
Zhili Feng	https://orcid.org/0009-0005-4273-0807
Lu Ma	https://orcid.org/0000-0001-5271-0686
Dinghua He	https://orcid.org/0009-0002-7961-7152
Lingyun Mei	https://orcid.org/0000-0003-3034-3322
Chufeng He	https://orcid.org/0000-0003-0327-3779
Yong Feng	https://orcid.org/0000-0003-3824-3780

AUTHOR CONTRIBUTIONS

Conceptualization: AC, YF, JL. Data curation: AC, CH, XP. Formal analysis: AC, XP, JS. Funding acquisition: YF, CH, LM (Lu Ma), JS, AC. Methodology: AC, XP, SZ, MQ, SM, YC. Project administration: JL, LM (Lingyun Mei), LM (Lu Ma). Visualization: AC, YB, XL, ZF, DH. Writing–original draft: AC, JL, LM (Lu Ma). Writing–review & editing: YF, CH.

SUPPLEMENTARY MATERIALS

Supplementary materials can be found online at https://doi.org/10.21053/ceo.2023.00668.

REFERENCES

1. Thienpont B, Dimitriadou E, Theodoropoulos K, Breckpot J, Fryssira H, Kitsiou-Tzeli S, et al. Refining the locus of branchio-otic syndrome 2 (BOS2) to a 5.25 Mb locus on chromosome 1q31.3q32.1. Eur J Med Genet. 2009 Nov-Dec;52(6):393-7.
2. Morisada N, Nozu K, Iijima K. Branchio-oto-renal syndrome: comprehensive review based on nationwide surveillance in Japan. Pediatr Int. 2014 Jun;56(3):309-14.
3. Unzaki A, Morisada N, Nozu K, Ye MJ, Ito S, Matsunaga T, et al. Clinically diverse phenotypes and genotypes of patients with branchio-oto-renal syndrome. J Hum Genet. 2018 May;63(5):647-56.
4. Fraser FC, Sproule JR, Halal F. Frequency of the branchio-oto-renal (BOR) syndrome in children with profound hearing loss. Am J Med Genet. 1980;7(3):341-9.
5. Kim HR, Song MH, Kim MA, Kim YR, Lee KY, Sonn JK, et al. Identification of a novel nonsynonymous mutation of EYA1 disrupting splice site in a Korean patient with BOR syndrome. Mol Biol Rep. 2014 Jul;41(7):4321-7.
6. Kochhar A, Orten DJ, Sorensen JL, Fischer SM, Cremers CW, Kimberling WJ, et al. SIX1 mutation screening in 247 branchio-oto-renal syndrome families: a recurrent missense mutation associated with BOR. Hum Mutat. 2008 Apr;29(4):565.
7. Zou D, Silvius D, Davenport J, Grifone R, Maire P, Xu PX. Patterning of the third pharyngeal pouch into thymus/parathyroid by Six and Eya1. Dev Biol. 2006 May;293(2):499-512.
8. Moody SA, LaMantia AS. Transcriptional regulation of cranial sensory placode development. Curr Top Dev Biol. 2015;111:301-50.
9. Shah AM, Krohn P, Baxi AB, Tavares AL, Sullivan CH, Chillakuru YR, et al. Six1 proteins with human branchio-oto-renal mutations differentially affect cranial gene expression and otic development. Dis Model Mech. 2020 Mar;13(3):dmm043489.
10. Chen A, Song J, Acke FR, Mei L, Cai X, Feng Y, et al. Otological manifestations in branchiootorenal spectrum disorder: a systematic review and meta-analysis. Clin Genet. 2021 Jul;100(1):3-13.
11. Song MH, Kwon TJ, Kim HR, Jeon JH, Baek JI, Lee WS, et al. Mutational analysis of EYA1, SIX1 and SIX5 genes and strategies for management of hearing loss in patients with BOR/BO syndrome. PLoS One. 2013 Jun;8(6):e67236.
12. Chang EH, Menezes M, Meyer NC, Cucci RA, Vervoort VS, Schwartz CE, et al. Branchio-oto-renal syndrome: the mutation spectrum in EYA1 and its phenotypic consequences. Hum Mutat. 2004 Jun;23(6):582-9.
13. Ruf RG, Xu PX, Silvius D, Otto EA, Beekmann F, Muerb UT, et al. SIX1 mutations cause branchio-oto-renal syndrome by disruption of EYA1-SIX1-DNA complexes. Proc Natl Acad Sci U S A. 2004 May;101(21):8090-5.
14. Gettelfinger JD, Dahl JP. Syndromic hearing loss: a brief review of common presentations and genetics. J Pediatr Genet. 2018 Mar;7(1):1-8.
15. Abdelhak S, Kalatzis V, Heilig R, Compain S, Samson D, Vincent C, et al. A human homologue of the Drosophila eyes absent gene underlies branchio-oto-renal (BOR) syndrome and identifies a novel gene family. Nat Genet. 1997 Feb;15(2):157-64.
16. Propst EJ, Blaser S, Gordon KA, Harrison RV, Papsin BC. Temporal bone findings on computed tomography imaging in branchio-oto-renal syndrome. Laryngoscope. 2005 Oct;115(10):1855-62.
17. Feng H, Xu H, Chen B, Sun S, Zhai R, Zeng B, et al. Genetic and phenotypic variability in Chinese patients with branchio-oto-renal or branchio-oto syndrome. Front Genet. 2021 Nov;12:765433.
18. Sang S, Ling J, Liu X, Mei L, Cai X, Li T, et al. Proband whole-exome sequencing identified genes responsible for autosomal recessive nonsyndromic hearing loss in 33 Chinese nuclear families. Front Genet. 2019 Jul;10:639.
19. Li H, Durbin R. Fast and accurate short read alignment with Burrows-Wheeler transform. Bioinformatics. 2009 Jul;25(14):1754-60.
20. Li H, Handsaker B, Wysoker A, Fennell T, Ruan J, Homer N, et al. The Sequence Alignment/Map format and SAMtools. Bioinformatics. 2009 Aug;25(16):2078-9.
21. Wang K, Li M, Hakonarson H. ANNOVAR: functional annotation of genetic variants from high-throughput sequencing data. Nucleic Acids Res. 2010 Sep;38(16):e164.
22. Johansson-Akhe I, Wallner B. Improving peptide-protein docking with AlphaFold-Multimer using forced sampling. Front Bioinform. 2022 Sep;2:959160.
23. Rentzsch P, Witten D, Cooper GM, Shendure J, Kircher M. CADD: predicting the deleteriousness of variants throughout the human genome. Nucleic Acids Res. 2019 Jan;47(D1):D886-94.
24. Ng PC, Henikoff S. Accounting for human polymorphisms predicted to affect protein function. Genome Res. 2002 Mar;12(3):436-46.
25. Richards S, Aziz N, Bale S, Bick D, Das S, Gastier-Foster J, et al. Standards and guidelines for the interpretation of sequence variants: a joint consensus recommendation of the American College of Medi-

cal Genetics and Genomics and the Association for Molecular Pathology. Genet Med. 2015 May;17(5):405-24.
26. Walker LC, Hoya M, Wiggins GA, Lindy A, Vincent LM, Parsons MT, et al. Using the ACMG/AMP framework to capture evidence related to predicted and observed impact on splicing: recommendations from the ClinGen SVI Splicing Subgroup. Am J Hum Genet. 2023 Jul;110(7):1046-67.
27. Stockley TL, Mendoza-Londono R, Propst EJ, Sodhi S, Dupuis L, Papsin BC. A recurrent EYA1 mutation causing alternative RNA splicing in branchio-oto-renal syndrome: implications for molecular diagnostics and disease mechanism. Am J Med Genet A. 2009 Mar; 149(3):322-7.
28. Orten DJ, Fischer SM, Sorensen JL, Radhakrishna U, Cremers CW, Marres HA, et al. Branchio-oto-renal syndrome (BOR): novel mutations in the EYA1 gene, and a review of the mutational genetics of BOR. Hum Mutat. 2008 Apr;29(4):537-44.
29. Vervoort VS, Smith RJ, O'Brien J, Schroer R, Abbott A, Stevenson RE, et al. Genomic rearrangements of EYA1 account for a large fraction of families with BOR syndrome. Eur J Hum Genet. 2002 Nov; 10(11):757-66.
30. Clarke JC, Honey EM, Bekker E, Snyman LC, Raymond RM Jr, Lord C, et al. A novel nonsense mutation in the EYA1 gene associated with branchio-oto-renal/branchiootic syndrome in an Afrikaner kindred. Clin Genet. 2006 Jul;70(1):63-7.
31. Mann N, Braun DA, Amann K, Tan W, Shril S, Connaughton DM, et al. Whole-exome sequencing enables a precision medicine approach for kidney transplant recipients. J Am Soc Nephrol. 2019 Feb;30(2): 201-15.
32. Krug P, Moriniere V, Marlin S, Koubi V, Gabriel HD, Colin E, et al. Mutation screening of the EYA1, SIX1, and SIX5 genes in a large cohort of patients harboring branchio-oto-renal syndrome calls into question the pathogenic role of SIX5 mutations. Hum Mutat. 2011 Feb;32(2):183-90.
33. Kwon MJ, Boo SH, Kim HJ, Cho YS, Chung WH, Hong SH. A novel splice site mutation in the EYA1 gene in a Korean family with branchio-oto (BO) syndrome. Acta Otolaryngol. 2009 Jun;129(6):688-93.
34. Chen P, Liu H, Lin Y, Xu J, Zhu W, Wu H, et al. EYA1 mutations leads to Branchio-Oto syndrome in two Chinese Han deaf families. Int J Pediatr Otorhinolaryngol. 2019 Aug;123:141-5.
35. Rickard S, Boxer M, Trompeter R, Bitner-Glindzicz M. Importance of clinical evaluation and molecular testing in the branchio-oto-renal (BOR) syndrome and overlapping phenotypes. J Med Genet. 2000 Aug;37(8):623-7.
36. Wang YG, Sun SP, Qiu YL, Xing QH, Lu W. A novel mutation in EYA1 in a Chinese family with Branchio-oto-renal syndrome. BMC Med Genet. 2018 Aug;19(1):139.
37. Henriksen AM, Tumer Z, Tommerup N, Tranebjaerg L, Larsen LA. Identification of a novel EYA1 splice-site mutation in a Danish branchio-oto-renal syndrome family. Genet Test. 2004 Winter;8(4):404-6.
38. Okada M, Fujimaru R, Morimoto N, Satomura K, Kaku Y, Tsuzuki K, et al. EYA1 and SIX1 gene mutations in Japanese patients with branchio-oto-renal (BOR) syndrome and related conditions. Pediatr Nephrol. 2006 Apr;21(4):475-81.
39. Sanggaard KM, Rendtorff ND, Kjaer KW, Eiberg H, Johnsen T, Gimsing S, et al. Branchio-oto-renal syndrome: detection of EYA1 and SIX1 mutations in five out of six Danish families by combining linkage, MLPA and sequencing analyses. Eur J Hum Genet. 2007 Nov;15(11): 1121-31.
40. Kim SH, Shin JH, Yeo CK, Chang SH, Park SY, Cho EH, et al. Identification of a novel mutation in the EYA1 gene in a Korean family with branchio-oto-renal (BOR) syndrome. Int J Pediatr Otorhinolaryngol. 2005 Aug;69(8):1123-8.
41. Gigante M, d'Altilia M, Montemurno E, Diella S, Bruno F, Netti GS, et al. Branchio-oto-renal syndrome (BOR) associated with focal glomerulosclerosis in a patient with a novel EYA1 splice site mutation. BMC Nephrol. 2013 Mar;14:60.
42. Castiglione A, Melchionda S, Carella M, Trevisi P, Bovo R, Manara R, et al. EYA1-related disorders: two clinical cases and a literature review. Int J Pediatr Otorhinolaryngol. 2014 Aug;78(8):1201-10.
43. Abdelhak S, Kalatzis V, Heilig R, Compain S, Samson D, Vincent C, et al. Clustering of mutations responsible for branchio-oto-renal (BOR) syndrome in the eyes absent homologous region (eyaHR) of EYA1. Hum Mol Genet. 1997 Dec;6(13):2247-55.
44. Kumar S, Kimberling WJ, Weston MD, Schaefer BG, Berg MA, Marres HA, et al. Identification of three novel mutations in human EYA1 protein associated with branchio-oto-renal syndrome. Hum Mutat. 1998;11(6):443-9.
45. Rodriguez-Soriano J, Vallo A, Bilbao JR, Castano L. Branchio-oto-renal syndrome: identification of a novel mutation in the EYA1 gene. Pediatr Nephrol. 2001 Jul;16(7):550-3.
46. Jaganathan K, Kyriazopoulou Panagiotopoulou S, McRae JF, Darbandi SF, Knowles D, Li YI, et al. Predicting splicing from primary sequence with deep learning. Cell. 2019 Jan;176(3):535-48.
47. Ratnadiwakara M, Mohenska M, Anko ML. Splicing factors as regulators of miRNA biogenesis: links to human disease. Semin Cell Dev Biol. 2018 Jul;79:113-22.
48. Mango R, Biocca S, del Vecchio F, Clementi F, Sangiuolo F, Amati F, et al. In vivo and in vitro studies support that a new splicing isoform of OLR1 gene is protective against acute myocardial infarction. Circ Res. 2005 Jul;97(2):152-8.
49. Wang SH, Wu CC, Lu YC, Lin YH, Su YN, Hwu WL, et al. Mutation screening of the EYA1, SIX1, and SIX5 genes in an East Asian cohort with branchio-oto-renal syndrome. Laryngoscope. 2012 May;122(5): 1130-6.
50. Lindau TA, Cardoso AC, Rossi NF, Giacheti CM. Anatomical changes and audiological profile in branchio-oto-renal syndrome: a literature review. Int Arch Otorhinolaryngol. 2014 Jan;18(1):68-76.
51. Kozlowski DJ, Whitfield TT, Hukriede NA, Lam WK, Weinberg ES. The zebrafish dog-eared mutation disrupts eya1, a gene required for cell survival and differentiation in the inner ear and lateral line. Dev Biol. 2005 Jan;277(1):27-41.
52. Christophorou NA, Bailey AP, Hanson S, Streit A. Activation of Six1 target genes is required for sensory placode formation. Dev Biol. 2009 Dec;336(2):327-36.
53. Soni UK, Roychoudhury K, Hegde RS. The Eyes Absent proteins in development and in developmental disorders. Biochem Soc Trans. 2021 Jun;49(3):1397-408.
54. Chen R, Amoui M, Zhang Z, Mardon G. Dachshund and eyes absent proteins form a complex and function synergistically to induce ectopic eye development in Drosophila. Cell. 1997 Dec;91(7):893-903.
55. Ohto H, Kamada S, Tago K, Tominaga SI, Ozaki H, Sato S, et al. Cooperation of six and eya in activation of their target genes through nuclear translocation of Eya. Mol Cell Biol. 1999 Oct;19(10):6815-24.
56. Musharraf A, Kruspe D, Tomasch J, Besenbeck B, Englert C, Landgraf K. BOR-syndrome-associated Eya1 mutations lead to enhanced proteasomal degradation of Eya1 protein. PLoS One. 2014 Jan;9(1): e87407.
57. Kalatzis V, Sahly I, El-Amraoui A, Petit C. Eya1 expression in the developing ear and kidney: towards the understanding of the pathogenesis of Branchio-Oto-Renal (BOR) syndrome. Dev Dyn. 1998 Dec;213(4):486-99.
58. Xu PX, Adams J, Peters H, Brown MC, Heaney S, Maas R. Eya1-deficient mice lack ears and kidneys and show abnormal apoptosis of organ primordia. Nat Genet. 1999 Sep;23(1):113-7.
59. Zheng Z, Wei X, Hildebrandt A, Schmidt B. A computational method for studying the relation between alternative splicing and DNA methylation. Nucleic Acids Res. 2016 Jan;44(2):e19.
60. Brzovic PS, Heikaus CC, Kisselev L, Vernon R, Herbig E, Pacheco D,

et al. The acidic transcription activator Gcn4 binds the mediator subunit Gal11/Med15 using a simple protein interface forming a fuzzy complex. Mol Cell. 2011 Dec;44(6):942-53.
61. Hafiz A, Bakri R, Alsaad M, Fetni OM, Alsubaihi LI, Shamshad H. In silico prediction of Plasmodium falciparum cytoadherence inhibitors that disrupt interaction between gC1qR-DBLβ12 complex. Pharmaceuticals (Basel). 2022 May;15(6):691.
62. Srivastava I, Misra SK, Bangru S, Boateng KA, Soares JA, Schwartz-Duval AS, et al. Complementary oligonucleotide conjugated multicolor carbon dots for intracellular recognition of biological events. ACS Appl Mater Interfaces. 2020 Apr;12(14):16137-49.
63. Ipsaro JJ, Huang L, Mondragon A. Structures of the spectrin-ankyrin interaction binding domains. Blood. 2009 May;113(22):5385-93.
64. Patrick AN, Cabrera JH, Smith AL, Chen XS, Ford HL, Zhao R. Structure-function analyses of the human SIX1-EYA2 complex reveal insights into metastasis and BOR syndrome. Nat Struct Mol Biol. 2013 Apr;20(4):447-53.
65. Goren A, Kim E, Amit M, Vaknin K, Kfir N, Ram O, et al. Overlapping splicing regulatory motifs: combinatorial effects on splicing. Nucleic Acids Res. 2010 Jun;38(10):3318-27.
66. Yang JY, Wang WQ, Han MY, Huang SS, Wang GJ, Su Y, et al. Addition of an affected family member to a previously ascertained autosomal recessive nonsyndromic hearing loss pedigree and systematic phenotype-genotype analysis of splice-site variants in MYO15A. BMC Med Genomics. 2022 Nov;15(1):241.
67. Gimsing S, Dyrmose J. Branchio-oto-renal dysplasia in three families. Ann Otol Rhinol Laryngol. 1986 Jul-Aug;95(4 Pt 1):421-6.
68. Cremers CW, Marres HA, Brunner HG. Neo-oval window technique and myringo-chorda-vestibulopexy in the BOR syndrome. Laryngoscope. 1993 Oct;103(10):1186-9.
69. Li HX, Zhou P, Tong M, Zheng Y. Branchial cleft fistula to branchio-oto-renal syndrome: a case report and literature review. J Int Med Res. 2020 Jul;48(7):300060520926363.
70. Nam DW, Kang DW, Lee SM, Park MK, Lee JH, Oh SH, et al. Molecular genetic etiology and revisiting the middle ear surgery outcomes of branchio-oto-renal syndrome: experience in a tertiary referral center. Otol Neurotol. 2023 Jun;44(5):e319-27.